AUT Journal of Mechanical Engineering

AUT J. Mech. Eng., 5(4) (2021) 639-654
DOI: 10.22060/ajme.2021.19402.5947

# Series Flat Plate Pulsating Heat Pipe: Fabrication and Experimentation

A. H. Ekrami[1], M. Sabzpooshani[*1], M. B. Shafii[2]

[1] Department of Mechanical Engineering, University of Kashan, Kashan, Iran
[2]Department of Mechanical Engineering, Sharif University of Technology, Tehran, Iran

**ABSTRACT:** Pulsating Heat Pipes have recently become popular due to their capability in removing heat at higher rates, over short or long distances. Their passive operation and relative ease of manufacturing have been added to their popularity. In this study, a combination of two flat plate pulsating heat pipes in series configuration is proposed and their thermo-hydraulic behavior is investigated experimentally in vertical bottom heated mode. The series configuration provides the possibility of heat removal from the heat source within longer distances at acceptable efficiencies. Fluid type, filling ratios, and input powers were the factors chosen to study their influence on the operation of the setup. The results showed that the 60% filling ratio for the water filled channel together with the 40% filling ratio for the methanol filled channel present the lowest thermal resistance in the range of considered input powers. It was observed that for all of the filling ratio combinations used, the methanol channel started oscillation before the water channel and it presented lower thermal resistance as compared with the water channel. The experimental results demonstrated that the dominant hydrodynamic fluid pattern is slug flow with the pulsation of fluid columns together with sporadic circulation at higher input power rates.

**Review History:**

Received: Dec.25, 2020
Revised: Apr. 06, 2021
Accepted: Apr. 07, 2021
Available Online:Apr. 18, 2021

**Keywords:**

Heat transfer
Heat pipe
Pulsation
Flow characteristics
Thermal resistance

## 1- Introduction

In search for more viable and efficient methods for management of thermal energy in different technological applications, the Heat Pipes took the attention of some thermal scientists as early as 1944 [1] and were further developed later on in the 1960s [2-4]. The Pulsating Heat Pipe (PHP), also known as Oscillating Heat Pipe, as a variant of the known heat pipes, was first invented by Akachi [5] in 1990. He describes the apparatus as a structure of loop-type heat pipe in which a heat carrying fluid circulates in a loop form in itself under its own vapor pressure within an elongated pipe so as to repeat vaporization and condensation, thus carrying out heat transfer. PHP is basically a meandering capillary tube which is partially filled with a proper heat conducting fluid. If the diameter of the tube is small enough, fluid is distributed inside it in the form of liquid slugs and vapor plugs. One characteristic that makes PHPs distinct from conventional heat pipes is the lack of wick structure. In conventional heat pipes, the wick is needed to sustain the cycle of evaporation and condensation. In PHPs, the capillary tube itself takes the role of the wick and retains the cycle through the capillarity action together with other thermo-physical factors.

Conceptually, a PHP has to have two regions in order to be able to function as an autonomous heat transport device. These include the heater and the condenser region. The working fluid keeps receiving heat and evaporating in the evaporator section and dissipating thermal energy and condensing in the condenser section. There may be a third section that connects the two stated sections together and is usually called the adiabatic section. The presence of this latter section is normally imposed by the requirement of separation of heat source and heat sink in practical applications and otherwise, it is not needed. When the temperature difference between evaporator and condenser regions exceeds a threshold, an oscillatory motion develops with liquid slugs and vapor bubbles, reciprocating between the heater and condenser regions. When sufficient thermal energy is absorbed, the slug-plug train may penetrate the two regions and create an intermittent circulatory motion.

PHPs are typically developed in closed-loop or open-loop configuration [6-9]. In the former, the two ends of the serpentine capillary tube are connected together, making a closed loop, while in the latter, the two ends are not directly connected, but are normally attached to a reservoir. The enhanced thermal performance of PHPs has been corroborated in many of the recent studies [10]. The influential factors that are studied, cover multitude of aspects including the structure of the apparatus, the working fluids, the Filling Ratio (FR), and the orientation of the setup [11-16]. Different materials

*Corresponding author's email: spooshan@kashanu.ac.ir

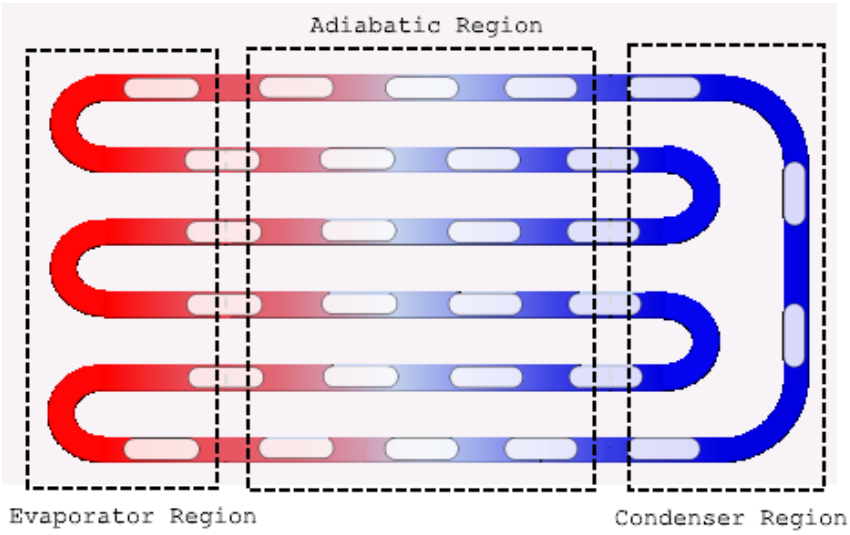


**Fig. 1. Schematic view of a PHP with three regions: Evaporator, Adiabatic, and Condenser**

have been utilized for the fabrication of PHPs, including metal, glass, and polymeric materials [11, 17-20]. Also, a variety of geometries have been tried to investigate the effect of channel shapes and cross-sections on the thermal performance of the device [16, 21]. Some researchers have considered novel configurations to increase thermal performance. For instance, Aboutalebi et al. [22] fabricated a rotary PHP in which the heat pipe rotates about its central axis and this helps to increase the thermal performance and operating range of the heat spreader. A radial but non-rotating PHP was also studied by Kelly et al. [23]. Qu et al. [20] performed experiments on the thermal performance of a three-dimensional multi-layered PHP. Bastakoti et al. [24] performed a comprehensive survey on the results of experimental and numerical works in recent years. Earlier works are reviewed and their results are tabulated by Zhang and Faghri [25].

The aim of this study is to investigate the influence of filling ratios, working fluids, and applied heating loads on the thermal performance of a novel Series Flat Plate Pulsating Heat Pipe (SFPPHP) and to study the fluid flow regimes evolved during the tests. This is the first time, to the best knowledge of the authors, that such a configuration is used in the fabrication of a Flat Plate Pulsating Heat Pipe (FPPHP). Due to the ease of use and cost effectiveness, aluminum is adopted as the base material for the fabrication of the SFPPHP.

Whereas coupling a PHP in series with another one is expected to increase the thermal resistance of the setup, the ultimate goal in this study is not particularly to maximize the thermal performance but to study the behavior of the series PHP while using different working fluids in the upper and lower channels. The series configuration may be helpful in situations where the heat dissipation location is far from the heat source and the PHP needs to go through a path that makes the fabrication of the setup too cumbersome, if possible at all. Even if successfully manufactured, its operation cannot be guaranteed and an ad hoc design is needed for any application, which makes the use of PHP economically less competitive. In such situations, two separate PHPs, with common and well-studied structures, may be connected in series using a well-insulated proper conducting medium which can be flexible enough to pass through any unusual path without adding unnecessary complexity to the design. Another situation which may make the series design is when the working fluid is harmful to the health and the environment and has to be kept under strict supervision. One such case is cooling the spent fuel pool of nuclear reactors where the working fluid will become radioactive after being exposed to the radiation of the nuclear fuel. In this case, the primary PHP, which will contain radioactive working fluid, is physically separated from the second PHP that is far from the radiation sources, through the usage of a series configuration. This will eliminate the chances of the release of radioactive fluid into the environment in case the primary PHP channels are damaged. Moreover, a series PHP configuration increases the overall degree of freedom in the design, providing more flexibility in the selection and tuning of the design parameters. For example, adoption of different working fluids, application of different vacuum pressures for each PHP, using different channel geometry and number of turns, etc.

**Table 1. Thermophysical properties of saturated water and saturated liquid methanol**

| | $(^{o}C)T$ | $\rho$ (kg/m$^3$) | (J/Kg.K) $C_p$ | $k$ (W/m.K) | $\sigma$ (N/m) |
|---|---|---|---|---|---|
| **Water** | 30 | 995.7 | 4183 | 0.603 | 0.07119 |
| | 50 | 988 | 4181 | 0.6305 | 0.06794 |
| | 70 | 977.7 | 4178 | 0.6495 | 0.06448 |
| | 100 | 958.4 | 4220 | 0.6651 | 0.05891 |
| | 110 | 951.0 | 4230 | 0.6676 | 0.05696 |
| **Methanol** | 30 | 782 | 2560 | 0.203 | 0.0218 |
| | 50 | 764 | 2700 | 0.202 | 0.0201 |
| | 70 | 746 | 2880 | 0.201 | 0.0185 |
| | 100 | 714 | 3180 | 0.198 | 0.0156 |
| | 110 | 704 | 3290 | 0.197 | 0.0146 |

The working fluid of the upper PHP, i.e. the one that is farther from the heat source, should have a lower boiling point with respect to the lower one to make the series PHP operable (see Fig. 4). This is needed because the working fluid after condensation in the condenser section of the lower PHP, transfers part of its thermal energy to the working fluid of the upper PHP through the upper evaporator region, i.e. the region next to the lower condenser region and farther from the heater block. This is accompanied by a temperature gradient starting with higher values in the first evaporator region and ending with lower values in the condenser section of the first PHP. Consequently, the working fluid of the upper PHP should have a boiling point that is lower enough compared with the condensation point of the lower PHP working fluid, so as to make the functioning of the SFPPHP possible. In this study, distilled water and 99.9% methanol are selected as working fluids for the lower and upper PHP, respectively. One reason for this selection is the high specific heat capacities of the two fluids which improve the overall thermal efficiency of the PHP. The boiling point of methanol boiling point, 64.7°C, is lower enough when compared with that of water, 100°C, satisfying the design requirement stated above. Both are non-toxic and stable under room temperature and pressure, making their handling convenient and requiring no special measures. In the designated operating temperature range and duration, the two fluids do not chemically react with Aluminum, the material selected for the base piece of the SFPPHP. They can be purchased at low prices and high purities. Moreover, they have been already widely used in many experiments [24, 25], proving their versatility for this application. Some of the thermos-physical properties of water and methanol are summarized in Table 1.

## 2- Experiment Setup

The SFPPHP schematic is shown in Fig. 2. The two pictures show the Front view (left) and the Back view (right) of the base plate on which the channels and holes are machined.

The layout of the test setup is schematically shown in Fig. 3. The condenser block is cooled by water with a constant temperature and flow rate. The heater is connected to an AC power supply. The temperature at different locations is measured using K-type thermocouples and recorded by a data logger at the rate of 1 Hz. The evacuation of PHP channels and injection of the working fluids is performed through a copper pipe, 1.5 mm ID, which is welded to a threaded headpiece. The headpiece is then fastened and sealed to the injection/suction hole on the back of the base plate. The evacuation of channels is done using a rotary vacuum pump, down to a pressure of 10 Pa [26-29]. At proper times, the phenomena inside the PHP channels are recorded by the camera. The setup and equipment are shown in Fig. 4.

In order to be operable in an oscillatory mode, a PHP should have channels with hydraulic diameter not exceeding a critical size, $D_{crit}$, which follows the relation:

$$D_{crit} = n.\sqrt{\frac{\sigma}{g\left(\rho_f - \rho_g\right)}} \tag{1}$$

where $\sigma$, $\rho_f$, and $\rho_g$ are surface tension, liquid density, and vapor density of the working fluid, respectively. $g$ is the gravitational acceleration rate and $n$ is equal to 2. This relation is based on the definition of Bond number [30, 31]:

$$Bo^2 = \frac{D_H{}^2 g\left(\rho_f - \rho_g\right)}{\sigma} \tag{2}$$

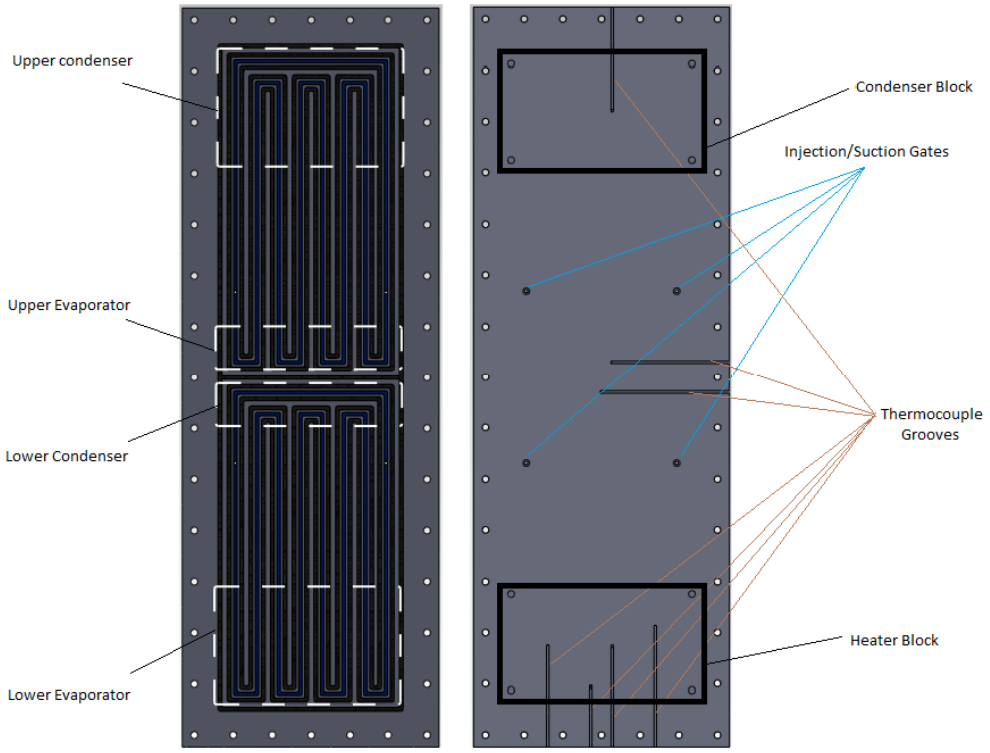


**Fig. 2. Series PHP Front view (left) and Back view (right).**

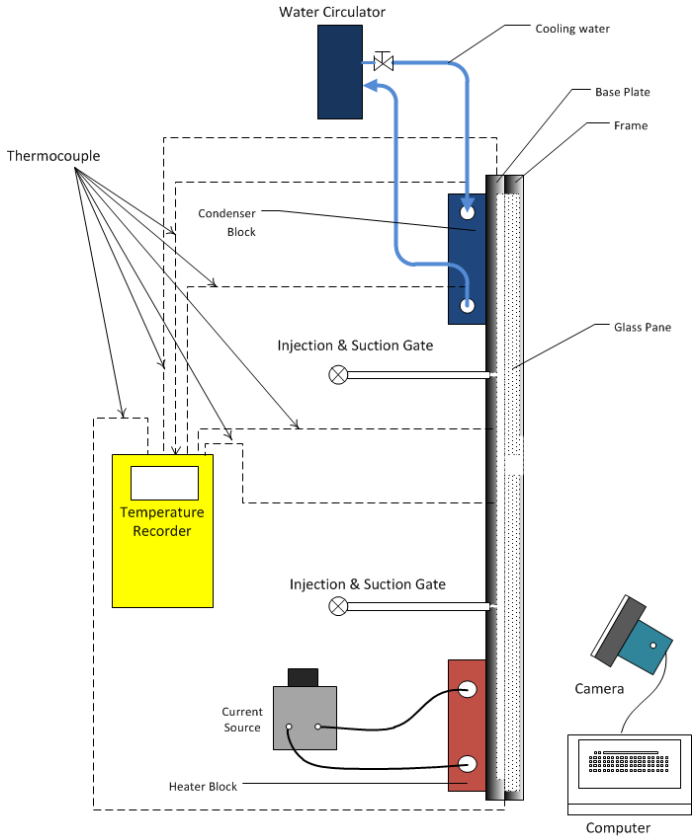


**Fig. 3. Schematic of SFPPHP and equipment**

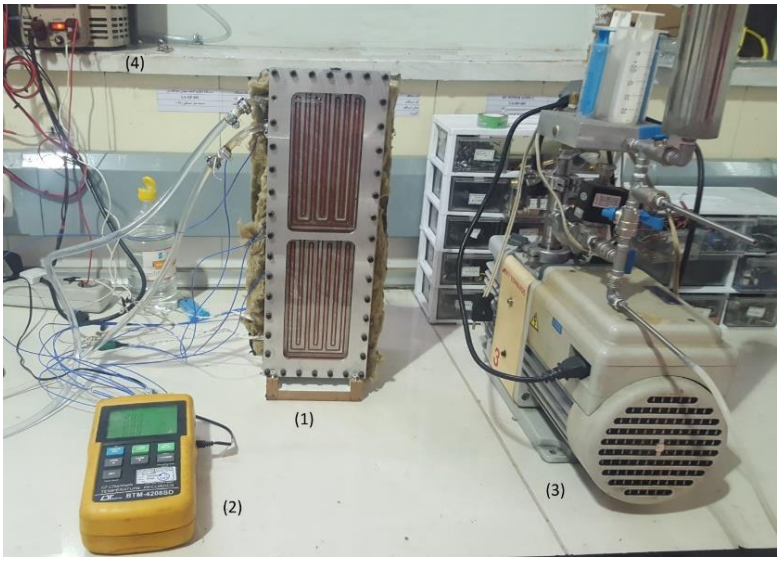


**Fig. 4. SFPPHP setup (1), temperature recorder (2), vacuum pump (3) and power source (4)**

**Table 2. Water and Methanol maximum capillary hydraulic diameters at 70^o C and 50^o C**

| | Temperature (°C) | Surface tension (N/m) | Liquid density (kg/m$^3$) | Vapor density (kg/m$^3$) | $D_{crit}$ (mm) |
|---|---|---|---|---|---|
| **Water** | 70 | 0.06448 | 977.7 | 0.198 | 5.2 |
| **Methanol** | 50 | 0.0201 | 764 | 0.39 | 3.3 |

which is the ratio of the body force to the surface tension. So, adopting a critical Bo equal to 2, we obtain the Eq. (1). Table 1 contains the thermophysical properties of saturated water and methanol at temperatures 30°C to 110°C. The calculated critical hydraulic diameters based on Eq. (1) are presented in Table 2. Critical diameters are calculated for the average temperatures of 70°C for water and 50°C for methanol so as to be more relevant in the working range of the PHPs. Inspecting Table 2, it is found that adopting $D_{crit}$ =2 mm should be a proper choice, being about 60% the size of the smaller capillary diameter.

The PHP base plate consists of a $430 \times 150 \times 10$ mm plate of aluminum on which two sets of meandering channels, each having four branches, are machined to contain the working fluids. The fluid channels have $2 \times 2$ mm square cross-section, resulting in a 2 mm hydraulic diameter. In order to provide a mechanism for sealing the fluid channels against ingress of fluid from one channel into adjacent channels and also keeping the negative pressure inside the channels, a series of grooves with proper sizes are machined around and between the fluid channels to contain silicone O-rings. These grooves are shown in black color in Fig. 2, left view. On the backside of the base plate, a number of grooves are foreseen for the thermocouples. At the end of each thermocouple groove, a hole is drilled so that its bottom is 1.5 mm away from the bottom of the fluid channel on the other side. This makes the tip of the thermocouple come as close as possible to the working fluid; providing a more precise measurement of working fluid temperature. Two holes provide the possibility of suction of air from inside the channels and injection/drainage of working fluids before/after each test. The heater is fabricated from an aluminum block $120 \times 70 \times 20$ mm (Fig. 5).

Two holes are drilled on one side face of the block and two cartridge type heaters are inserted inside the holes and connected to an electrical power supply. The condenser is fabricated from a similar aluminum block (Fig. 6). To provide efficient heat removal, a meandering channel is machined inside the block. Water enters

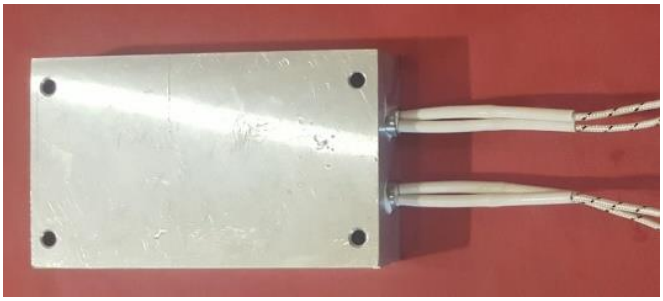

Fig. 5. Heater block with cartridge type electric heaters inserted

Fig. 6. Condenser block with the cap removed

through a hole from one end of the channel and exits through another hole on the other end. A 5 mm thick aluminum plate is used to cap the open channel. It is bolted to the block and water sealed using a silicone gasket. The heater and condenser blocks are bolted to the back of the base plate.

Heat resistant silicone O-rings with 1 mm OD are placed inside the grooves machined on the front face. The widths and depths of the grooves are calculated based on standard tables available for the design of vacuum sealing. As a rule of thumb, the height of these grooves should be 30% smaller and the width should be 20% larger than the O-ring diameter when a circular cross-section O-ring is used.

In order to provide visual access to the phase change phenomena evolving inside the SFPPHP channels, a tempered glass sheet is fitted inside a clamp frame which is firmly screwed to the front face of the base plate. To prevent direct contact between the glass and the aluminum clamp frame, a flat silicone gasket is placed inside the frame and then the glass sheet is fixed over the gasket. The series PHP module's back and sides are insulated using rock wool in order to minimize heat exchange with the ambient air.

The exploded view of the final assembly is demonstrated in Fig. 7. In this figure, the nuts and bolts and also the injection/evacuation pipes are not shown for more clarity of the figure.

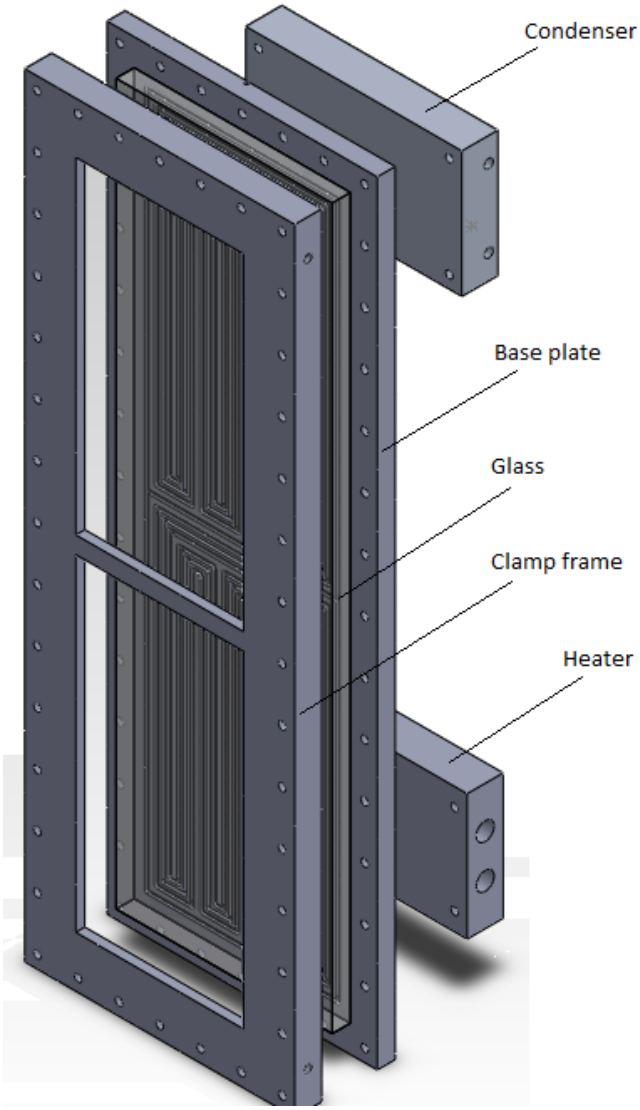


Fig. 7. Exploded view of the Series PHP assembly

## 3- Experiment Procedure

For working fluids, distilled water and non-degassed pure methanol are used, as discussed in Section 1. In order to remove non-condensable gases from water, it was left to freeze and melt a couple of times. The methanol used is 99.9% pure laboratory grade. Primarily, the lower PHP is evacuated to an absolute pressure of 10 Pa [32]. Then, the desired amount of working fluid is injected through a gastight syringe. The total volume of each series of meandering channels in the lower and upper parts of series PHP is 6 cc. The volume related to

evacuation/injection pipe and valves is around 0.5 cc. So, the whole volume of each part for the purpose of calculation of FR is taken to be 6.5 cc. Three FRs are chosen to investigate their influence on the operation and performance of the setup. These include 40%, 60%, and 80%. In this experiment, the lower PHP is partially filled with water, 60% by volume, and this FR is not modified for the rest of the tests. The upper PHP is then partially filled with methanol at three different FRs. Filling ratios are selected to cover the normal range of FRs used and reported in the vast majority of experimental studies performed by researchers, using different geometries and working fluids. Table 1 in [24] can be consulted for the most frequent FRs used. Accordingly, the three values selected for the methanol channel may well fit in the most popular range. For the water channel also these values could be adopted but having three FRs for each of the channels would require nine experiments, which takes into account that each experiment was repeated three times, to ensure its repeatability, the required number of experiments would add up to at least 27. The time and resources available did not allow the author to perform this number of attempts. So, to take a middle value, 60% FR was selected for the water channel for all of the tests. Adopting other FR values for the water channel and changing the methanol channel FR could be performed in subsequent research for the purpose of comparison with the results of this study.

The condenser block is fed with water and the setup is left for 10 minutes to reach a fairly steady temperature before connecting the power source to the heater block.

After the power source is connected to the heater, the voltage is regulated so that the desired power is obtained. To calculate the electric power generated in the cartridge type heaters, the relation is used, where $W$ is the generated power, $V$ is the voltage of the power source, and $I$ is the electric current. The electric current is measured using a clamp type multi-meter. A range of powers is used to cover the operating regime of the SFPPHP. The selected power values include 70, 100, 120, 150, 200, and 260 W. In-between every power rise, the phenomena occurring in the capillary channels are carefully observed and recorded by the camera.

The thermal resistance, R, of a PHP, is defined as the ratio of the temperature difference between the evaporator section and the condenser section to the thermal energy transferred to the evaporator section:

$$R = \frac{T_{evaporator} - T_{condenser}}{Q_{evaporator}} \tag{3}$$

As there are two sets of PHPs in series in the current design, two thermal resistances may be defined for each set:

$$R_{upper} = \frac{T^{upper}_{evaporator} - T^{upper}_{condenser}}{Q^{upper}_{evaporator}} \tag{4}$$

$$R_{lower} = \frac{T^{lower}_{evaporator} - T^{lower}_{condenser}}{Q^{lower}_{evaporator}} \tag{5}$$

where the upper and lower in these equations refer to the methanol and water filled channels in the current design (see Fig. 4). Because of non-ideal heat production in the available cartridge heaters, and also due to non-perfect contact between the heater block and the base plate, the distribution of temperature in the heater block is not homogenous. Hence, to get a better estimate of the working fluid temperature in the evaporator region, more than one thermocouple is installed under the heater block, measuring the temperature at different locations under the block (see Fig. 4, right view). The temperature of working fluid in the evaporator section is taken as the average of the temperatures measured by these thermocouples:

$$T_{evaporator} = \frac{\sum_{i=1}^{4} T^{i}_{evaporator}}{4} \tag{6}$$

In the other sections including the condenser section of the lower PHP, the evaporator section of the upper PHP, and the condenser section of the upper PHP only one thermocouple is used to measure the temperature. Two thermocouples are also used to measure the temperature of the water entering and exiting the condenser block.

As thermal resistance of the SFPPHP, it can be taken as the ratio of the temperature difference between the evaporator region under the heater block and the condenser region under the condenser block and the heat rate added through the heater block:

$$R_{total} = \frac{T^{lower}_{evaporator} - T^{upper}_{condenser}}{Q^{lower}_{evaporator}} \tag{7}$$

## 4- Uncertainty Analysis

To measure the uncertainty of the results of the performed experiments, the methodology suggested by Moffat [33] was applied. Accordingly, a variable $X_i$ that has a known uncertainty $\delta X_i$ is represented as

$$X_i = X_i\left(\text{measured}\right) \pm \delta X_i \tag{8}$$

The value $X_i$ (measured) represents the observed value in a single experiment or the average of observed values in a multiple-sample experiment. Taking an experiment $E$ to be a function of $n$ measured parameters $X_i$, then

$$E = E\left(X_1 X_2 \ldots, X_n\right) \tag{9}$$

For a single measurement, the influence on the uncertainty of the result would be

$$\delta E_{X_i} = \frac{\partial E}{\partial X_i}\delta X_i \tag{10}$$

Considering the effect of every measurement in the final result, the ultimate uncertainty in $E$ would be

$$\delta E = \left\{\sum_{i=1}^{N}\left(\frac{\partial E}{\partial X_i}\delta X_i\right)^2\right\}^{1/2} \tag{11}$$

If the uncertainty estimate is sought as a fraction of measurement and the result is expressible as a product of the underlying parameters, the ultimate uncertainty can be expressed as

$$\frac{\delta E}{E} = \left\{\sum_{i=1}^{N}\left(\frac{\delta X_i}{X_i}\right)^2\right\}^{1/2} \tag{12}$$

When considering Eq. (7) for the calculation of total thermal resistance of the apparatus, two parameters are distinguishable, $T$ and $Q$. As $Q$ is not directly measured but is calculated by measuring electricity current, $I$, and Voltage, $V$, and multiplying them, there will be three independent variables for uncertainty analysis, namely $T$, $I$ and $V$. The measurement uncertainties of the three variables are shown in Table 3.

They reflect the tolerances of the measuring devices used for reading and registering the variables. Table 4 presents the relative uncertainty in thermal resistance of the SFPPHP for the three FRs applied in this study.

It also includes the relative uncertainties in temperature and heat load. It should be noted that the three uncertainties reported in Table 4 under the header of $\delta T / \Delta T$ demonstrate the relative uncertainty of temperature measurement when considering the lower PHP, upper PHP, and the whole apparatus. But, when reporting the uncertainties under $\delta Q / Q$, only the last column which is related to the relative uncertainty in temperature difference between the lower evaporator and upper condenser is taken into account since Eq. (7) is applied in this study for the purpose of calculation of total thermal resistance. $\Delta Ts$ are the smallest temperature differences measures in each specific FR. This brings about the maximum uncertainty in temperature at each experiment. For the case of 60-80 FR, as an example, the calculations are performed as follows:

$$\delta T = 0.5,\ \Delta T = 26.5,\ \delta I = 0.1,\ \delta V = 0.5,\ \frac{\delta T}{\Delta T} = \frac{0.5}{26.6} = .019,$$

$$\frac{\delta Q}{Q} = \left(\left(\frac{\delta I}{I}\right)^{0.5} + \left(\frac{\delta V}{V}\right)^{0.5}\right)^{0.5} = \left(\left(\frac{0.1}{0.45}\right)^{0.5} + \left(\frac{0.5}{155}\right)^{0.5}\right)^{0.5} = 0.022,$$

$$\frac{\delta R}{R} = \left(\left(\frac{\delta T}{\Delta T}\right)^{0.5} + \left(\frac{\delta Q}{Q}\right)^{0.5}\right)^{0.5} = \left(0.019^{0.5} + 0.022^{0.5}\right)^{0.5} = 0.029$$

## 5- Results and Discussion

The experimental results are presented in two sections. At first, the flow characteristics of the novel configuration of PHPs are discussed and then the performances of the SFPPHP are presented and evaluated.

### 5- 1- Flow characteristics

In all of the three experiments, with the temperature increase in the evaporator region, bubbles start to appear at the bottom of the U-shaped channels or the feedback channel, connecting the first branch to the last one (in the water filled PHP) (see Fig. 8).

**Table 3. Uncertainties in measured variables Temperature, T, electrical current, I, and electrical voltage, V.**

| | $\delta T$ | $\delta I$ | $\delta V$ |
|---|---|---|---|
| **Uncertainty** | (K) ±0.5 | ±0.1 (A) | ±0.5 (V) |

**Table 4. Relative uncertainties in temperature, T, heat rate, Q, and thermal resistance, R**

| Filling Ratio | $\pm\frac{\delta T}{\Delta T}$ % | | | $\pm\frac{\delta Q}{Q}$ % | $\pm\frac{\delta R}{R}$ % |
|---|---|---|---|---|---|
| | Lower | Upper | Total | | |
| 60-60 | 2.6 | 4.6 | 1.7 | 4 | 4.4 |
| 60-40 | 2.9 | 5.1 | 1.8 | 2.2 | 2.8 |
| 60-80 | 3.1 | 1.0 | 1.9 | 2.2 | 2.9 |

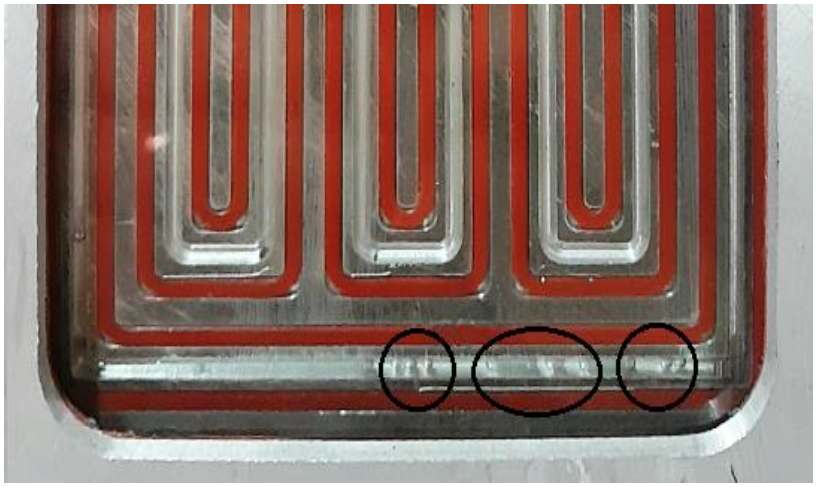

**Fig. 8. The appearance of bubbles in the feedback channel.**

This continues with an increase in the number of the bubbles and their subsequent coalescence to create larger ones. The process continues with detachment and slow oscillation of the elongated bubbles. Bubbles in the vertical channels usually appear close to the bottom of the PHP in the evaporator region. Like in the feedback channels, small bubbles detach from the wall and combine together to create larger ones. These larger elongated bubbles tend to float upwards towards the condenser region. At this moment, liquid columns are observed with bubbles below and above them in the evaporator and condenser regions, respectively. These columns, having different heights, vibrate slowly in place, without penetrating the condenser region (Fig. 9).

This is the dominant flow pattern up to the startup time when a sudden and short pulsation is observed in some capillary channels. This phenomenon occurs under the influence of the acceleration of bubble plugs from the evaporator and penetration into the condenser region. Usually, a reverse movement is observed in the adjacent column. But, at the same time, farther columns may show concurrent or counter-current fluid displacement. The methanol filled channel (upper PHP) was observed to be usually the first one to start oscillating. The nucleation sites appear more homogeneously in the upper PHP, within the U-turns located in the upper evaporator, compared with the lower PHP where the nucleation sites appear sporadically at the bottom of one U-bend and show up, with some delay, in other places in the lower evaporator. With further increase of the temperature, the explained process becomes faster and the production and breakage of vapor bubbles create a turbulent environment. In some columns, the vapor plugs move so harshly that push the liquid slugs above them to the condenser end of the PHP. The result can be intermittent circulation inside the channels. In practice, the dominant pattern observed at low and medium temperatures was the oscillation of the liquid slugs rather than the circulation of the train of bubble plugs and liquid slugs. The circulatory behavior was favored at higher temperatures/input power rates. Also, this behavior was observed to start earlier with the increase of the filling ratio. The difference between circulatory and oscillatory flow is demonstrated in Fig. 10.

**Fig. 9. Liquid-vapor menisci (denoted with circles) and the bubbles generating in the heater region (denoted by polygons) before the start-up of the PHP**

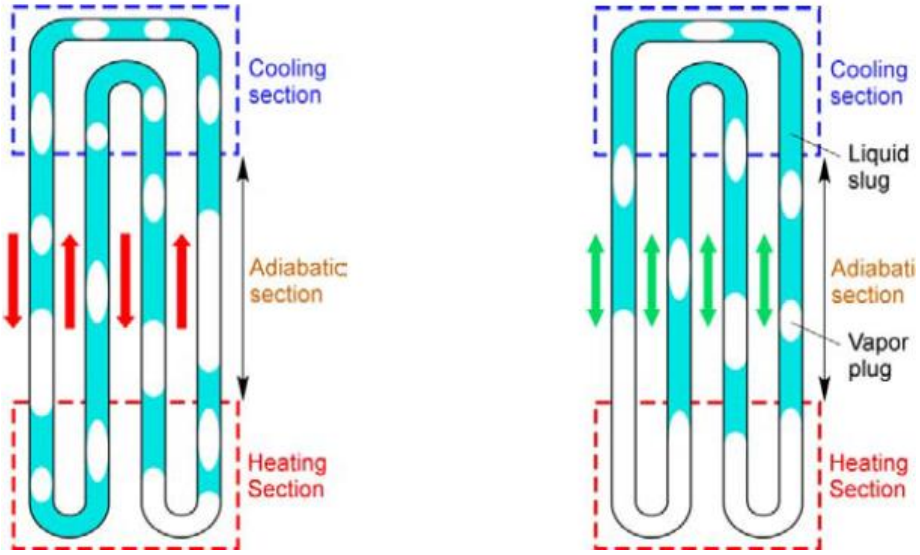


**Fig. 10. Motions of liquid slugs and vapor plugs in oscillating heat pipe [34]**

For the case of 60%-40%, the pulsation started during the 100 W input power application in both methanol and water channels. Pulsation was the only pattern observed in the methanol channels up to 200 W. But in the water PHP, it was observed only after applying 150 W input power. In the two other cases, the water PHP showed the same behavior, as expected, since its FR is the same in all experiments. The circulation in 60%-60% in methanol channels was observed at the final minutes of application of 150 W power input while in the case of 60%-80%, the circulatory pattern developed at the end of 120 W and the beginning of the 150 W input power application.

Different flow patterns were observed to occur under different conditions. Before the start of pulsation, no major bulk flow was observed in the channels. The only significant phenomenon was the appearance of small bubbles in the evaporator region, growing up and detaching from the capillary wall with the increase of local temperature. When the heat input rate was increased, nucleate boiling started near the U-bends which led to the creation of elongated bubbles in the adiabatic section. At this stage which coincides with the start of pulsation, a slug flow was established within the channels. The flow was not circulatory but a reciprocating movement with short amplitude was established in the branches where bubbles originating from the evaporator region tend to migrate toward the condenser region, coalescing with a larger bubble which oscillates in the condenser region, around the U-bend. By an increase in input power more energy will be induced into the fluid system, bubbles merge together and long bubble plugs appeared. At some instant, bubbles gained enough momentum to push the liquid slugs into the condenser region or penetrate through the liquid slugs and pass through the condenser U-bends. Semi-annular/Annular patterns were observed during this phase which is accompanied by an intermittent circulatory behavior. Comparing the water and methanol channels, no specific difference was observed as to the flow patterns and the oscillatory/circulatory behavior. The main difference was the time at which these patterns appeared. As discussed earlier, the methanol channel begins its oscillation before the water channel. It was observed that during higher power rates, oscillations inside the methanol channel presented higher frequencies and shorter amplitudes compared with the water channel. At the end of the power input rate, both channels show fast oscillation of bubble and liquid trains without a clear circulatory flow regime. Actually, partial dry out near the bottom of evaporator regions prevented the free circulation of fluid, expelling the vapor upward toward the condenser region. The prevailing flow pattern in the adiabatic region during this phase was annular flow. In the condenser region, an annular/semi-annular pattern was observed.

After the end of the experiments in vertical bottom heated mode, the SFPPHP was tested in the horizontal state, with the glass window facing upward and the apparatus back parallel to the ground. It was observed that the oscillation in water channels diminish abruptly and the PHP stopped operation. The methanol in the upper PHP showed a high frequency oscillation with a small amplitude and no circulatory flow could be distinguished. This was accompanied by a dry out in the evaporator region of both upper and lower PHPs. The total thermal resistance of the SFPPHP was measured which presented a sharp increase.

Table 5 provides the summary of the parameters chosen in this series of experiments.

### 5- 2- Performance evaluation

Three experiments were performed with three different filling ratios in methanol filled channel, including 40%, 60%, and 80%. The water filled channel had the same filling ratio of 60% in the three experiments. In each experiment, six different heat loads, including 70 W, 100 W, 120 W, 150 W, 200 W, and 260 W, were applied to the evaporator of the SFPPHP. The condenser was supplied with water at a flow rate equal to 0.185 lit/s. As shown in Fig. 11, the prevailing trend is a decrease in thermal resistance when increasing the heat input. For the case of 60%-60% filling ratios, after the initial rise to about 0.39, a constant decline in heat resistance is observed for the range of heat inputs. For the case of 60%-40%, there is a primary increase in heat resistance which tops at around 0.36 and then it starts decreasing. Applying more heat input makes the heat resistance for this case to continue decreasing and approach the same heat resistance as that of the 60%-60% case.

As can be observed from Fig. 11, the heat resistance for the heat loads 200 W and 260 W result in almost equal values for 60%-60% and 60%-40% FRs. For 60%-80% filling ratios, the behavior observed is similar to 60%-40% case, except that its maximum heat resistance is slightly lower and the heat resistance decreases at a smaller rate which causes the SFPPHP to attain higher resistances compared with the other two cases when increasing the heat load. Actually, the 60%-80% case achieves higher resistance values when the input heat rate surpasses around 140 W. To better understand the physics of the phenomena, the individual heat resistances of each lower (water filled) and upper (methanol filled) PHP is studied. It can be observed in Fig. 12 that the trend of changes in thermal resistance for the upper and lower PHPs in 60%-40% configuration follows the same trend observed for the total SFPPHP; rising rapidly to an early maximum and then starting to drop at a gentler rate.

Let's denote the applied input thermal energy rate by $Q$, the temperature difference between the evaporator and condenser regions of the lower and upper PHPs by

**Table 5. Summary of parameters used in the experiments**

| Parameter | | Value |
|---|---|---|
| Channel Hydraulic Diameter | | 2 mm |
| Aluminum Base Block Size | | 430×150×10 mm |
| Heater & Condenser Block Sizes | | 120×70×20 mm |
| O-ring diameter | | 1 mm |
| Depressurization inside channels | | 10 Pa |
| Total volume of each empty channel | | 6.5 cc |
| Filling Ratios | Methanol channel | 40%, 60%, 80% |
| | Water channel | 60% |
| Input Powers | | 70 W, 100 W, 120 W, 150 W, 200 W, 260 W |

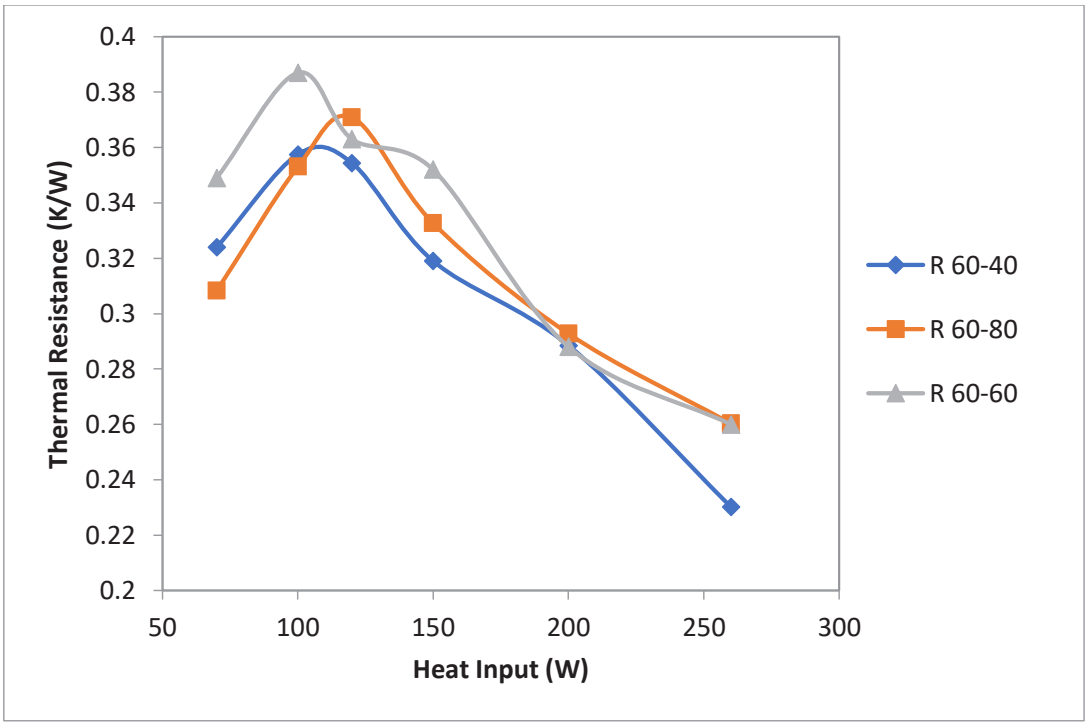


**Fig. 11. SFPPHP total thermal resistance vs. applied heat load**

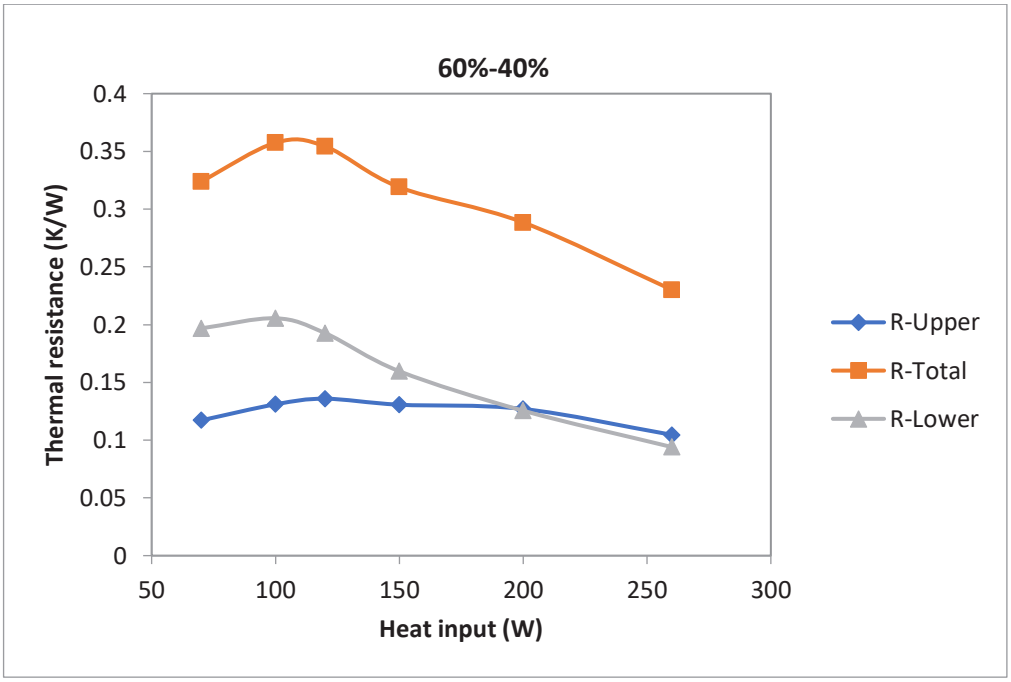


**Fig. 12. Thermal resistance vs. heat input of the lower part, the upper part, and the whole series PHP with filling ratios 60%-40%**

$\Delta T_L$ and $\Delta T_U$, and thermal resistance of the lower and upper PHPs by $R_L$ and $R_U$, respectively. Ignoring the heat loss during the heat transport from the lower to the upper PHP, the following relation must be valid:

$$Q = \frac{\Delta T_L}{R_L} = \frac{\Delta T_U}{R_U} \tag{13}$$

Despite the fact that the heater block is mounted on the lower PHP and this section experiences higher temperatures for the same input heat rates compared with the upper PHP, it was observed that the upper PHP always starts oscillating before the lower one. This is due to methanol being more volatile than water with a boiling point at atmospheric pressure equal to $64.7^{\circ}\mathrm{C}$, while that of water is $100^{\circ}\mathrm{C}$. So, in a specific time interval, the methanol channel is operating as a PHP while the water in lower channels is stagnant. PHP functioning causes a decrease in temperature difference between the cooler and the hotter section of the upper PHP, $\Delta T_U$. At the same time, because the lower PHP is not functioning, the heat spreading is not achieved as efficiently as in the upper PHP and a steeper $\Delta T_L$ is observed. As the heat input rate, $Q$, is the same for both channels, a smaller thermal resistance for the upper PHP ($R_U$) must be obtained compared with the lower PHP ($R_L$). This explains the lower $R_U$ vs. $R_L$ in most of the working range in three experiments depicted in Fig. 12 to Fig. 14. The initial rise in thermal resistance before reaching the peak value is the result of one or both of the PHPs being non-operational at that temperature. Because water and methanol have higher specific heats relative to Aluminum and also since working fluids heat of vaporization necessitate higher input power for the PHP to start up, these parameters appear as extra resistances which cause the PHP thermal resistance to rising before the start-up.

While the heat of vaporization manifests itself as a thermal resistance during the non-operational phase, after the pulsation of liquid slugs starts in the channels, it contributes to heat transport by delivering more thermal energy to the condenser section and absorbing more thermal energy in the evaporator section which causes a better heat dissipation and decrease in temperature gradient. Consequently, a working fluid with higher latent heat should cause a lower thermal resistance after the start of pulsations.

The competing factors explained above result in thermal resistance curves of the lower and upper PHPs to cross at temperatures which bias to the higher input powers. Inspecting Figs. 12 to 14, it can be observed that this intersection point is around 200 W for 60%-40% and 60%-80% setups while for the 60%-60% case, it occurs at smaller input power, approximately 185 W.

Returning to Fig. 11, it can be observed that the intersection point for the total thermal resistances also locates around 200 W. Although there is a touchpoint here, where curves converge close to that point and

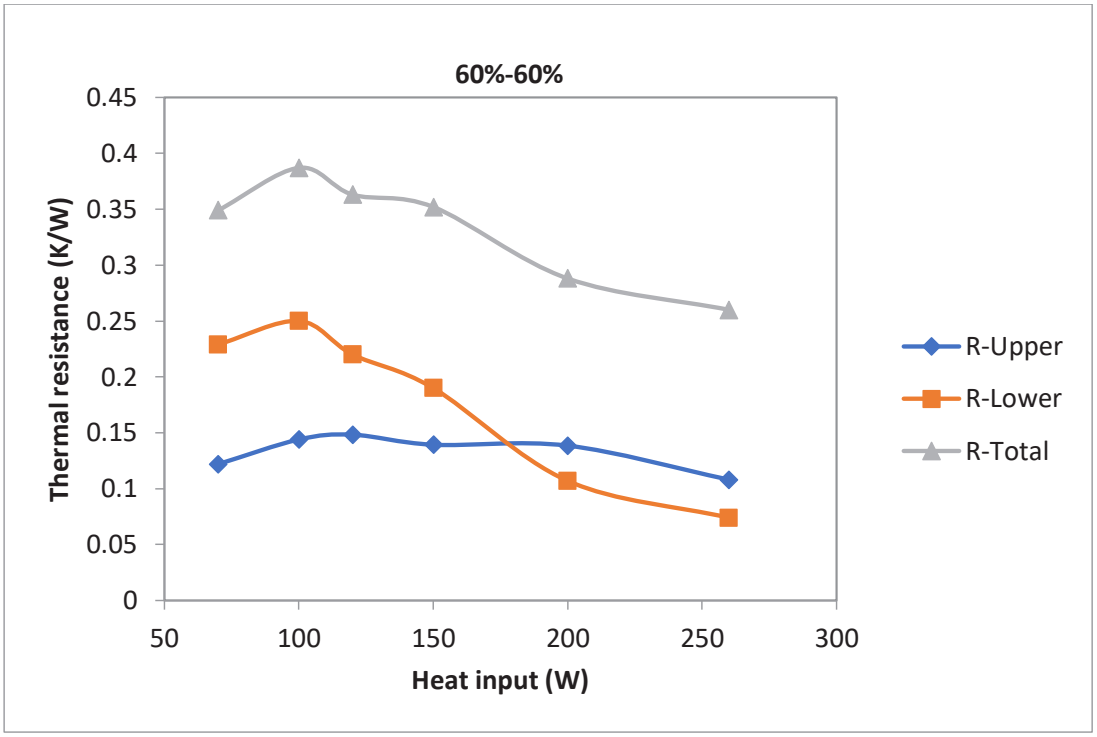


**Fig. 13. Thermal resistance vs. heat input of the lower part, the upper part, and the whole series PHP with filling ratios 60%-60%**

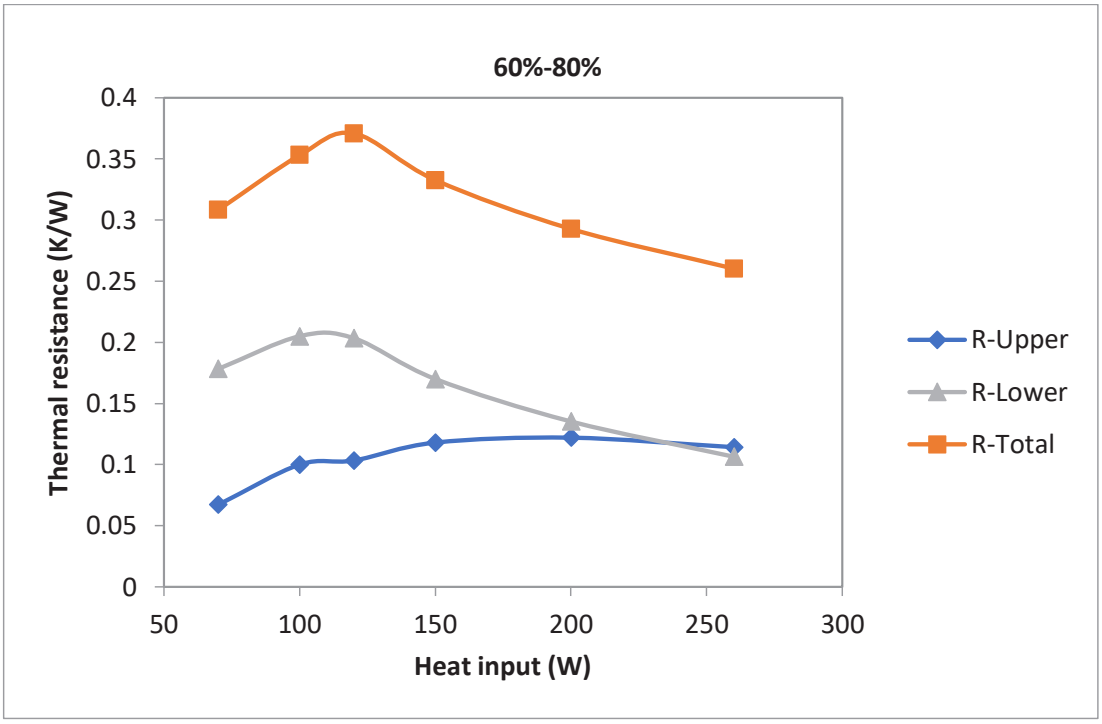


**Fig. 14. Thermal resistance vs. heat input of the lower part, the upper part, and the whole Series PHP with filling ratios 60%-80%**

begin to diverge afterward. Another point that may be considered is that the 60%-40% setup has the lowest overall thermal resistance among the three experiments. Except for the starting input power where the 60%-80% setup has a smaller thermal resistance, for the rest of the working range, the 60%-40% configuration keeps it superiority in terms of the smaller magnitude of thermal resistance.

## 6- Conclusions

In the present study, an aluminum flat plate pulsating heat pipe was manufactured using a series configuration. The effect of filling ratios and fluid types on the operation and performance of the total configuration was investigated. The following conclusions may be drawn from the study:

I. With water in the lower PHP and methanol in the upper PHP, as working fluids, the thermal resistance of the SFPPHP when applying 60% FR for the lower one and 40% for the upper one is the lowest compared with the two other FR options used.

II. The 60-80 and 60-60 FR configurations have comparable heat resistances in the whole range of tests. Meanwhile, the 60-60 FR shows higher thermal resistances up to around 180W input power. From that power up, the 60-80 FR presents marginally higher resistances.

III. The thermal resistance in every three FR options tends to rapidly decrease with an increase in input power rate.

IV. Based on the observations, the upper PHP always shows lower thermal resistances in low to medium input heat rates when compared with the lower PHP. The thermal resistance of the lower PHP drops below that of the upper PHP for higher input heat rates.

V. The dominant flow behavior during the operation of the SFPPHP in both upper and lower PHPs is an oscillatory movement of bubbles and liquid slugs, rather than a circulatory flow.

VI. The apparatus stops operating in horizontal inclination. At this orientation, the evaporator sections dry out and short amplitude fast oscillations are observed in the adiabatic section.

VII. The SFPPHP manifests a thermal behavior similar to conventional flat plate PHPs in terms of its thermal resistance response.

## Acknowledgments

The authors acknowledge the support of the department of mechanical engineering of Sharif University of Technology for providing the laboratory and instruments for performing the experiments. Special thanks to Mr. Zarei and Mr. Jafari for their interest and kind assistance in developing the experimental setups and supporting the activities.

## Nomenclature

| | |
|---|---|
| (Specific heat capacity, J/(kg. K | $C_p$ |
| Diameter, m | D |
| Gravitational acceleration, m/s$^2$ | g |
| Electrical current, A | I |
| Thermal resistance, K/W | R |
| Electrical voltage, V | V |
| Greek symbols | |
| Kinematic viscosity, N.s/m$^2$ | $\mu$ |
| Density, kg/m$^3$ | $\rho$ |
| Surface tension, N/m | $\sigma$ |
| Subscript | |
| Critical | crit |
| Liquid | f |
| Gas | g |
| Hydraulic | H |

## References

[1] R. Gaugler, Heat transfer device, in: U.S. Patent No. 2350348, 1994.

[2] L. Trefethen, On the surface tension pumping of liquids or a possible role of the candlewick in space exploration, GE Tech. Info., Serial, (615) (1962) D114.

[3] T. Wyatt, Satellite temperature stabilization system, in: U.S. Patent No. 3090212, 1963.

[4] G. Grover, T. Cotter, G. Erickson, Structures of very high thermal conductance, Journal of Applied Physics, 35(6) (1964) 1990-1991.

[5] H. Akachi, Structure of heat pipe, in: U.S. Patent No. 4921041, 1990.

[6] P. Charoensawan, S. Khandekar, M. Groll, P. Terdtoon, Closed loop pulsating heat pipes: Part A: parametric experimental investigations, Applied thermal engineering, 23(16) (2003) 2009-2020.

[7] Y. Zhang, A. Faghri, Heat transfer in a pulsating heat pipe with open end, International Journal of Heat and Mass Transfer, 45(4) (2002) 755-764.

[8] R.T. Dobson, Theoretical and experimental modelling of an open oscillatory heat pipe including gravity, International Journal of Thermal Sciences, 43(2) (2004) 113-119.

[9] S. Khandekar, M. Groll, P. Charoensawan, S. Rittidech, P. Terdtoon, Closed and open loop pulsating heat pipes, in: K-4, Proceedings of 13th International Heat Pipe Conference, China Academy of Space Technology Shanghai, China, 2004.

[10] E. Jiaqiang, X. Zhao, H. Liu, J. Chen, W. Zuo, Q. Peng, Field synergy analysis for enhancing heat transfer

capability of a novel narrow-tube closed oscillating heat pipe, Applied Energy, 175 (2016) 218-228.

[11] M. Ebrahimi, M.B. Shafii, M.A. Bijarchi, Experimental investigation of the thermal management of flat-plate closed-loop pulsating heat pipes with interconnecting channels, Applied Thermal Engineering, 90 (2015) 838-847.

[12] C.-Y. Tseng, K.-S. Yang, K.-H. Chien, M.-S. Jeng, C.-C. Wang, Investigation of the performance of pulsating heat pipe subject to uniform/alternating tube diameters, Experimental thermal and fluid science, 54 (2014) 85-92.

[13] B.S. Taft, A.D. Williams, B.L. Drolen, Review of pulsating heat pipe working fluid selection, Journal of Thermophysics and Heat Transfer, 26(4) (2012) 651-656.

[14] X. Wang, L. Jia, Experimental study on heat transfer performance of pulsating heat pipe with refrigerants, Journal of Thermal Science, 25(5) (2016) 449-453.

[15] V. Manno, M. Mameli, S. Filippeschi, M. Marengo, Thermal instability of a Closed Loop Pulsating Heat Pipe: Combined effect of orientation and filling ratio, (2014).

[16] B. Borgmeyer, C. Wilson, R. Winholtz, H. Ma, D. Jacobson, D. Hussey, Heat transport capability and fluid flow neutron radiography of three-dimensional oscillating heat pipes, Journal of Heat Transfer, 132(6) (2010).

[17] T. Hao, H. Ma, X. Ma, Heat transfer performance of polytetrafluoroethylene oscillating heat pipe with water, ethanol, and acetone as working fluids, International Journal of Heat and Mass Transfer, 131 (2019) 109-120.

[18] W. Kim, S.J. Kim, Effect of a flow behavior on the thermal performance of closed-loop and closed-end pulsating heat pipes, International Journal of Heat and Mass Transfer, 149 (2020) 119251.

[19] A. Takawale, S. Abraham, A. Sielaff, P.S. Mahapatra, A. Pattamatta, P. Stephan, A comparative study of flow regimes and thermal performance between flat plate pulsating heat pipe and capillary tube pulsating heat pipe, Applied Thermal Engineering, 149 (2019) 613-624.

[20] J. Qu, J. Zhao, Z. Rao, Experimental investigation on the thermal performance of three-dimensional oscillating heat pipe, International Journal of Heat and Mass Transfer, 109 (2017) 589-600.

[21] H. Alijani, B. Çetin, Y. Akkuş, Z. Dursunkaya, Effect of design and operating parameters on the thermal performance of aluminum flat grooved heat pipes, Applied Thermal Engineering, 132 (2018) 174-187.

[22] M. Aboutalebi, A.N. Moghaddam, N. Mohammadi, M. Shafii, Experimental investigation on performance of a rotating closed loop pulsating heat pipe, International communications in heat and mass transfer, 45 (2013) 137-145.

[23] B. Kelly, Y. Hayashi, Y.J. Kim, Novel radial pulsating heat-pipe for high heat-flux thermal spreading, International Journal of Heat and Mass Transfer, 121 (2018) 97-106.

[24] D. Bastakoti, H. Zhang, D. Li, W. Cai, F. Li, An overview on the developing trend of pulsating heat pipe and its performance, Applied Thermal Engineering, 141 (2018) 305-332.

[25] Y. Zhang, A. Faghri, Advances and unsolved issues in pulsating heat pipes, Heat Transfer Engineering, 29(1) (2008) 20-44.

[26] B. Zohuri, Application of Heat Pipes to Fissionable Nuclear Reactor, in: Heat Pipe Applications in Fission Driven Nuclear Power Plants, Springer, 2019, pp. 219-264.

[27] R. Hernandez, M. Todosow, N.R. Brown, Micro heat pipe nuclear reactor concepts: Analysis of fuel cycle performance and environmental impacts, Annals of Nuclear Energy, 126 (2019) 419-426.

[28] M. Mochizuki, R. Singh, T. Nguyen, T. Nguyen, S. Sugihara, K. Mashiko, Y. Saito, V. Wuttijumnong, Nuclear reactor must need heat pipe for cooling, Frontiers in Heat Pipes (FHP), 2(3) (2012).

[29] P.-f. Gou, L.E. Fennern, C.D. Sawyer, Nuclear reactor heat pipe, in: U.S. Patent No. 5684848, 1997.

[30] H. Akachi, F. Polášek, P. Štulc, Pulsating heat pipes, in: Proceedings 5th International Heat Pipe Symp., 1996, 1996.

[31] Q. Cai, C.-l. Chen, J.F. Asfia, Operating characteristic investigations in pulsating heat pipe, (2006).

[32] Edwards Vacuum Pump Manual, in: Instruction Manual: RV3, RV5, RV8 and RV12 Rotary Vane Pumps.

[33] R.J. Moffat, Describing the uncertainties in experimental results, Experimental thermal and fluid science, 1(1) (1988) 3-17.

[34] R. Senjaya, T. Inoue, Bubble generation in oscillating heat pipe, Applied thermal engineering, 60(1-2) (2013) 251-255.

**HOW TO CITE THIS ARTICLE**

*A. H. Ekrami, M. Sabzpooshani, M. B. Shafii, Series Flat Plate Pulsating Heat Pipe: Fabrication and Experimentation, AUT J. Mech Eng., 5 (4) (2021) 639-654.*

**DOI:** 10.22060/ajme.2021.19402.5947